Introduction to Multicopter Design and Control

Lesson 07 Sensor Calibration and Measurement Model

Quan Quan , Associate Professor

qq_buaa@buaa.edu.cn

BUAA Reliable Flight Control Group, http://rfly.buaa.edu.cn/

Beihang University, China

北航可靠飞行控制研究组

BUAA Reliable Flight Control Group

Outline

1. Three-Axis Accelerometer
2. Three-Axis Gyroscope
3. Three-Axis Magnetometer
4. Ultrasonic Range Finder
5. Barometer
6. 2D Laser Range Finder
7. GPS
8. Camera
9. Brief Summary

1. Three-Axis Accelerometer

☐ Fundamental Principle

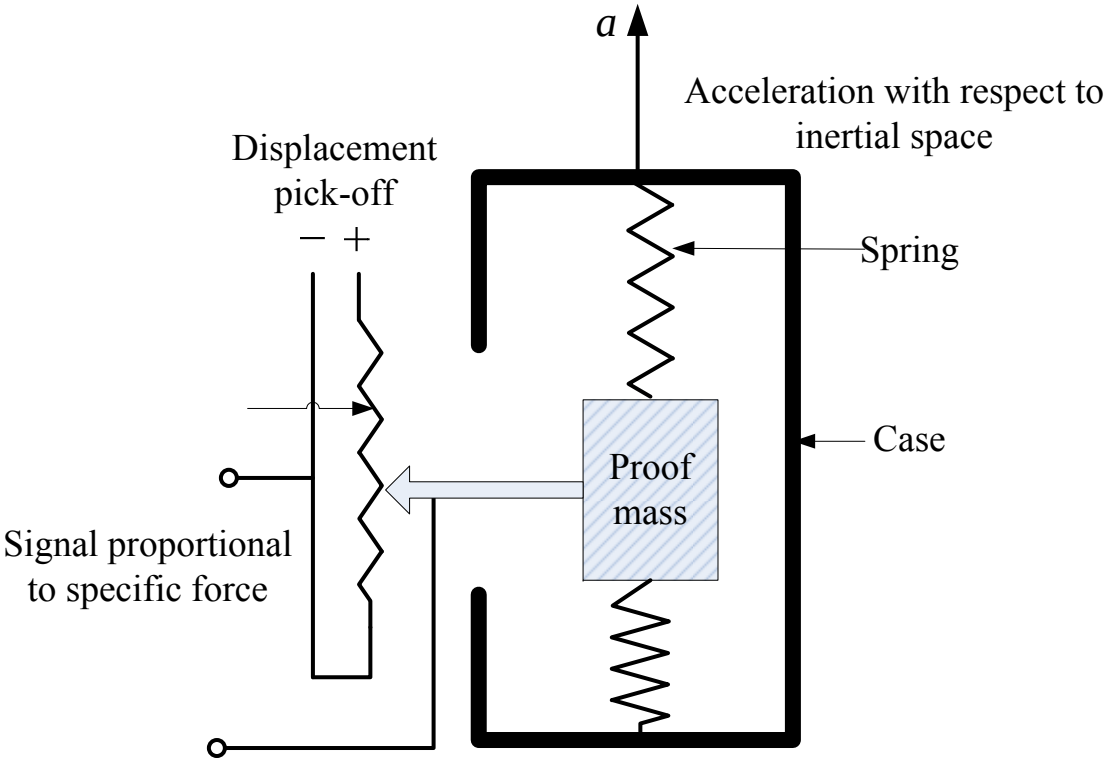

Figure 7.1 Accelerometer which measures the specific force

The three-axis accelerometer is a kind of inertial sensor which measures the specific force, namely the total acceleration eliminating gravity or the non-gravitational force per unit mass. When an accelerometer stays still, the acceleration of gravity can be sensed by the accelerometer, where the total acceleration is zero. In free-fall, the total acceleration is the acceleration of gravity, but the three-axis accelerometer will output zero.

1. Three-Axis Accelerometer

☐ Fundamental Principle

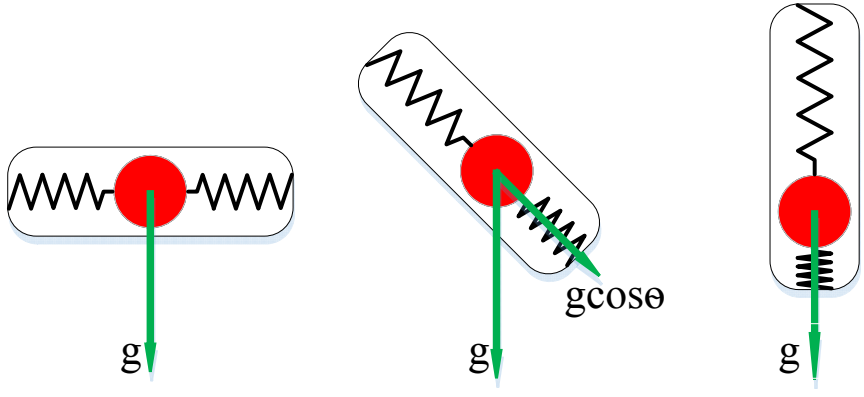

(a)Indicating value is 0 (b)Indicating value is gcosθ (c)Indicating value is g

Figure 7.2 Measuring principle of MEMS accelerometers

The principle of a three-axis accelerometer can be used to measure angles. Intuitively, as shown, the compression of spring is determined by the angle of the accelerometer to the ground. The specific force can be measured by spring compression length. Therefore, in the absence of external force, the accelerometer can accurately measure the pitch angle and roll angle, with zero cumulative error.

1. Three-Axis Accelerometer

☐ Fundamental Principle

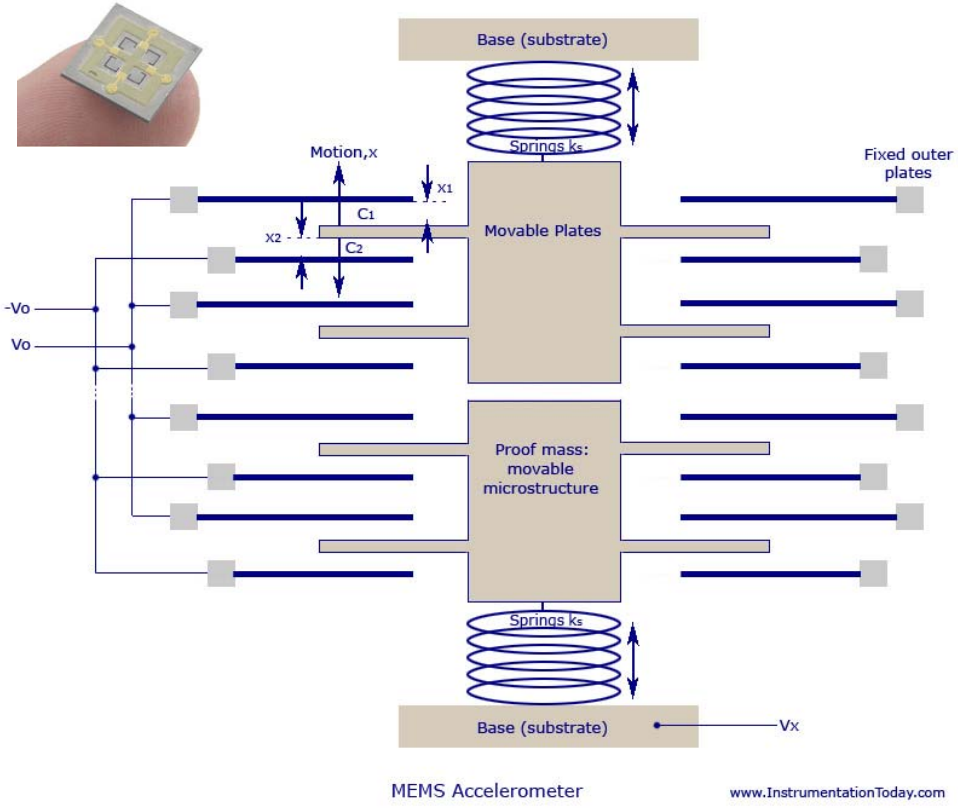

MEMS three-axis accelerometer is based on piezoresistive effect, piezoelectric effect or capacitive principle, the acceleration of those effects are proportional to resistance, voltage or capacitance, respectively. These values can be collected through the amplification circuit and filter circuit. The shortcoming of this sensor is that its output error induced by vibration is large.

Figure 7.3 Measuring principle of MEMS gyroscope, from http://www.instrumentationtoday.com/mems-accelerometer/2011/08/

1. Three-Axis Accelerometer

☐ Calibration

(1) Calibration

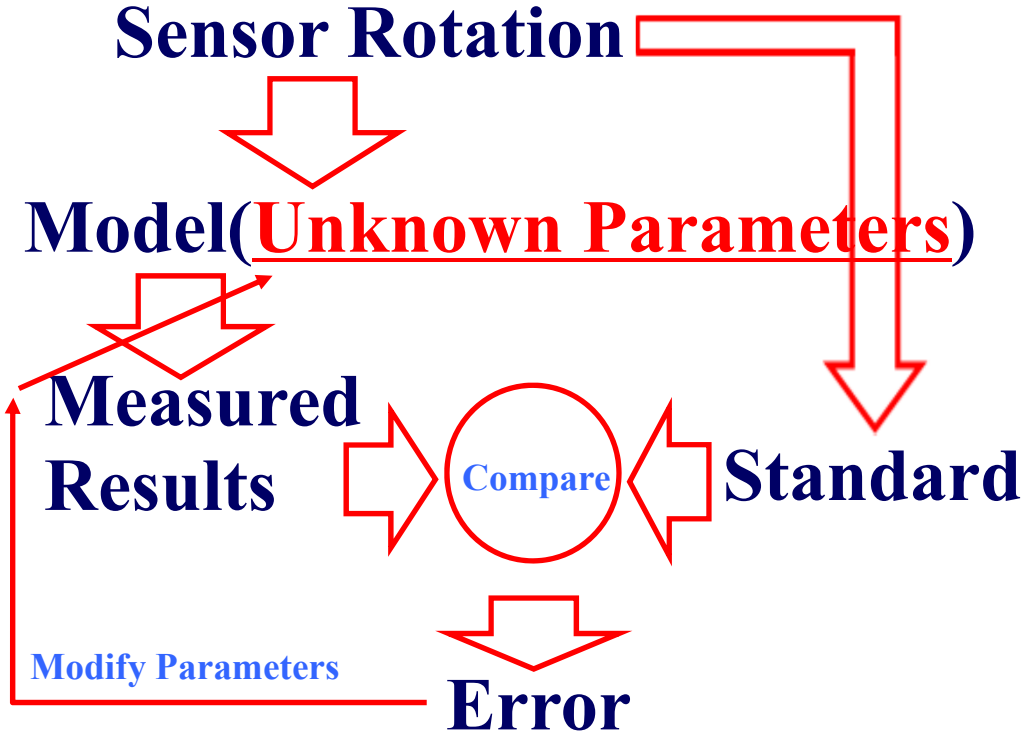

Figure 7.4 Calibration Principle of Accelerometer

1. Three-Axis Accelerometer

☐ Calibration

(2) Automatic Calibration

- General calibration: need external calibration equipment, but accurate.
- Automatic calibration: do not require external calibration devices, simple, slightly poor precision

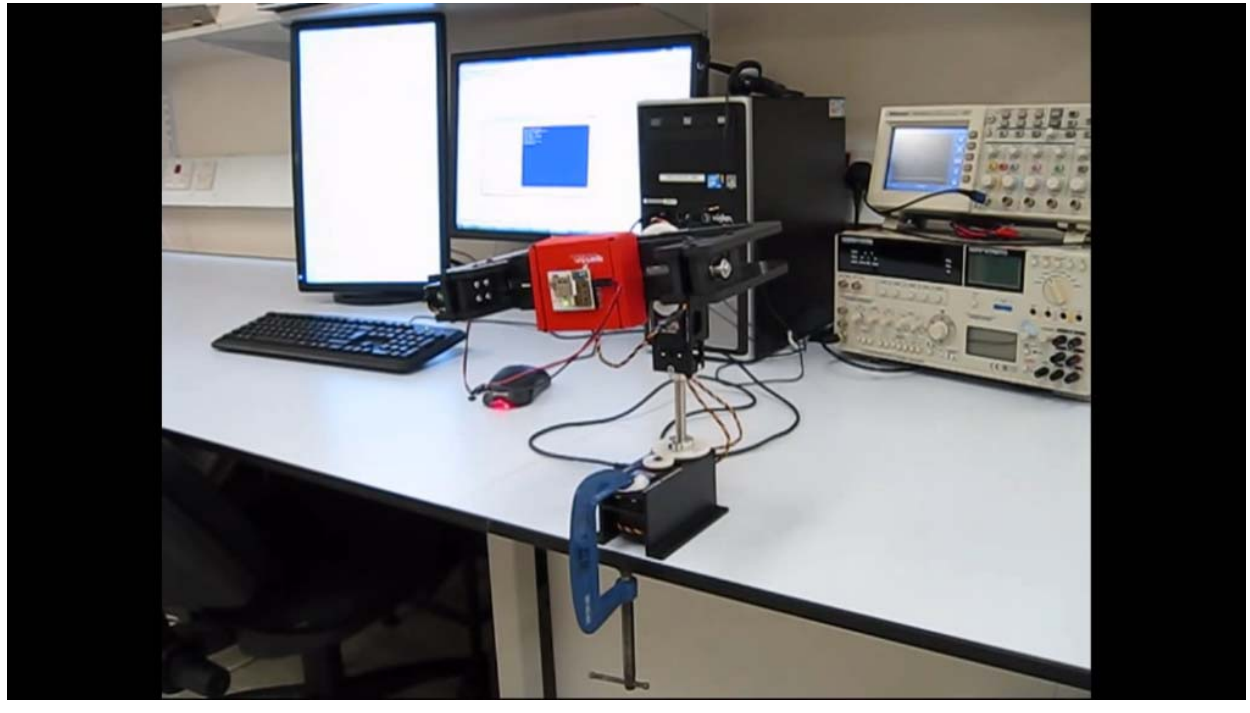

Accelerometer, magnetometer & gyroscope calibration
https://youtu.be/XqQCbkncVYI

1. Three-Axis Accelerometer

☐ Automatic Calibration[1],[2]

(1) Error Model

There exist some errors in the production and installation process of three-axis accelerometer. Thus the calibration process is needed. The error model is shown as follows:

$$ {}^{b}\mathbf{a}_{m} = \mathbf{T}_{a}\mathbf{K}_{a}\left({}^{b}\mathbf{a}'_{m} + \mathbf{b}'_{a}\right) $$

Calibrated acceleration

$$ \mathbf{T}_{a} = \begin{bmatrix} 1 & \Delta\psi_{a} & -\Delta\theta_{a} \\ -\Delta\psi_{a} & 1 & \Delta\phi_{a} \\ \Delta\theta_{a} & -\Delta\phi_{a} & 1 \end{bmatrix} \quad \mathbf{K}_{a} = \begin{bmatrix} s_{ax} & 0 & 0 \\ 0 & s_{ay} & 0 \\ 0 & 0 & s_{az} \end{bmatrix} \quad \mathbf{b}'_{a} = \begin{bmatrix} b'_{ax} \\ b'_{ay} \\ b'_{az} \end{bmatrix} $$

Tiny tilt

Scale factor

Acceleration without calibration

bias

1. Three-Axis Accelerometer

☐ Automatic Calibration

(2) Calibration Principle

In order to calibrate an accelerometer, the following unknown parameters need to be estimated.

$$\Theta_{\mathrm{a}} = \begin{bmatrix} \Delta\psi_{\mathrm{a}} & \Delta\theta_{\mathrm{a}} & \Delta\phi_{\mathrm{a}} & s_{\mathrm{ax}} & s_{\mathrm{ay}} & s_{\mathrm{az}} & b'_{\mathrm{ax}} & b'_{\mathrm{ay}} & b'_{\mathrm{az}} \end{bmatrix}^{\mathrm{T}}$$

Define the following function

$${}^{\mathrm{b}}\mathbf{a}_{\mathrm{m}} = \mathbf{h}_{\mathrm{a}}\left(\Theta_{\mathrm{a}}, {}^{\mathrm{b}}\mathbf{a}'_{\mathrm{m}}\right) = \mathbf{T}_{\mathrm{a}}\mathbf{K}_{\mathrm{a}}\left({}^{\mathrm{b}}\mathbf{a}'_{\mathrm{m}} + \mathbf{b}'_{\mathrm{a}}\right)$$

Principle: Regardless of the location of the accelerometer placed, its value should always be constant, that is, the actual size of the local gravity vector.

According to this principle, we have

$$\Theta_{\mathrm{a}}^{*} = \arg\min_{\Theta_{\mathrm{a}}} \sum_{k=1}^{M} \left(\left\| \mathbf{h}_{\mathrm{a}}\left(\Theta_{\mathrm{a}}, {}^{\mathrm{b}}\mathbf{a}'_{\mathrm{m},k}\right) \right\| - \mathrm{g} \right)^{2}$$

arg min {} represent the value getting minimum value of objective function

1. Three-Axis Accelerometer

☐ Automatic Calibration

(3) Calibration Results

- Data sources: IMU in the PIXHAWK4, data is collected through analyzing Mavlink protocol via a series bus.

- Calibration result:

$$\mathbf{T}_a = \begin{bmatrix} 1 & 0.0093 & -0.0136 \\ -0.0093 & 1 & 0.0265 \\ 0.0136 & -0.0265 & 1 \end{bmatrix}, \mathbf{K}_a = \begin{bmatrix} 1.0203 & 0 & 0 \\ 0 & 1.0201 & 0 \\ 0 & 0 & 1.0201 \end{bmatrix}, \mathbf{b}'_a = 10^{-5} \begin{bmatrix} -2.755 \\ 1.565 \\ -9.942 \end{bmatrix}$$

1. Three-Axis Accelerometer

☐ Automatic Calibration

(3) Calibration Results

$$\text{Dist}=\left(\left\|\mathbf{h}_{\mathrm{a}}\left(\Theta_{\mathrm{a}},{}^{\mathrm{b}}\mathbf{a}'_{\mathrm{m},k}\right)\right\|-\mathrm{g}\right)^2$$

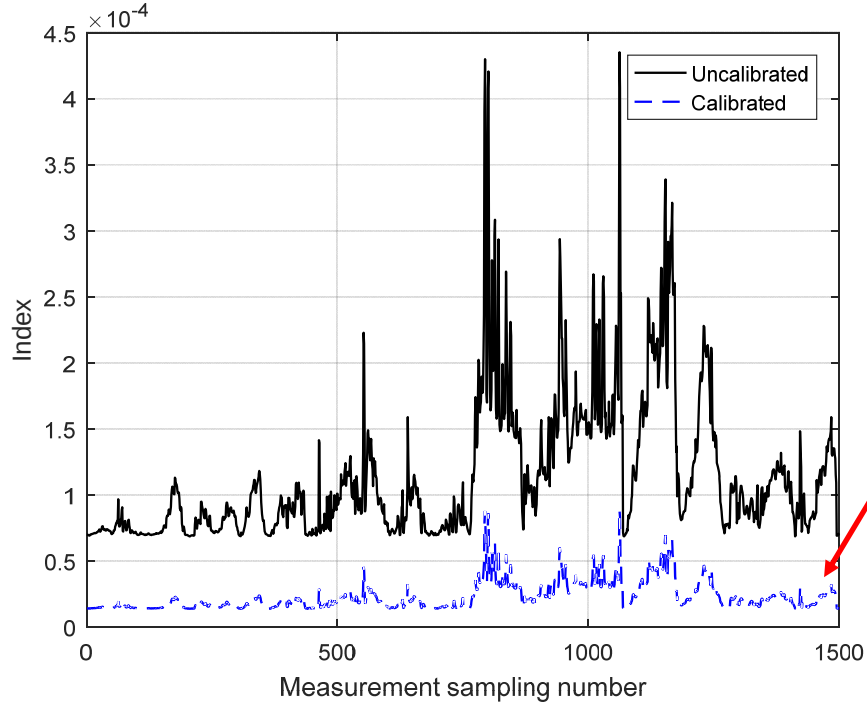

The error become smaller after calibration

Figure 7.5 Accelerometer Calibration Error

1. Three-Axis Accelerometer

☐ Measurement Model

MEMS accelerometers are fixed to the Aircraft-Body Coordinate Frame(ABCF), which can measure specific force along different axes. The measurement ${}^{b}\mathbf{a}_m \in \mathbb{R}^3$ is denoted as:

$$ {}^{b}\mathbf{a}_m = {}^{b}\mathbf{a} + \mathbf{b}_a + \mathbf{n}_a $$

Calibrated Acceleration

Real Acceleration

Drift

Gaussian White Noise

Since most MEMS sensors are produced by semiconductor material which is sensitive to temperature. And installation, circuit design factors are also able to produce errors. Thus, zero drift and temperature drift are inevitable.

Drift $\mathbf{b}_a$ can be modeled as Gaussian random process.

$$ \dot{\mathbf{b}}_a = \mathbf{n}_{\mathbf{b}_a} $$

And $\mathbf{n}_{\mathbf{b}_a} \in \mathbb{R}^3$ is Gaussian white noise.

2.Three-Axis Gyroscope

☐ Fundemental Principle

Coriolis force:

When mass moves relative to the inertial system in a straight line, the trajectory of the mass is a curve, due to the inertia. Based on the rotation system, we believe that there is a force to drive the particle motion trajectory to form a curve. Coriolis force is a description of this offset, expressed as F= -2$m\omega \times$ v

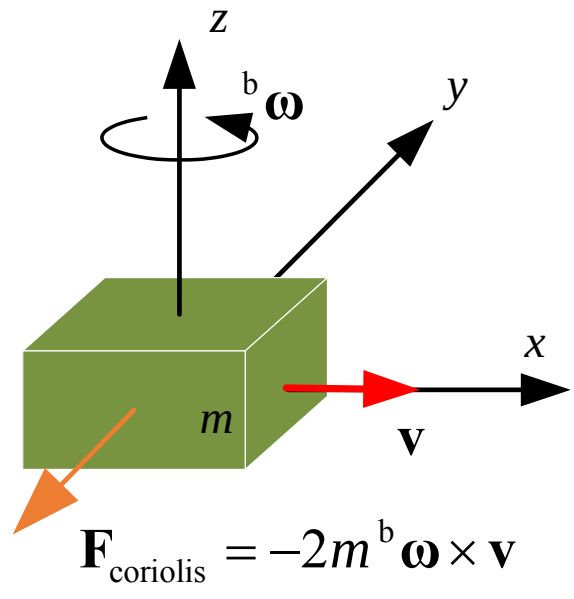

Figure 7.6 Fundemental Principle of Coriolis force

2.Three-Axis Gyroscope

☐ Fundemental Principle

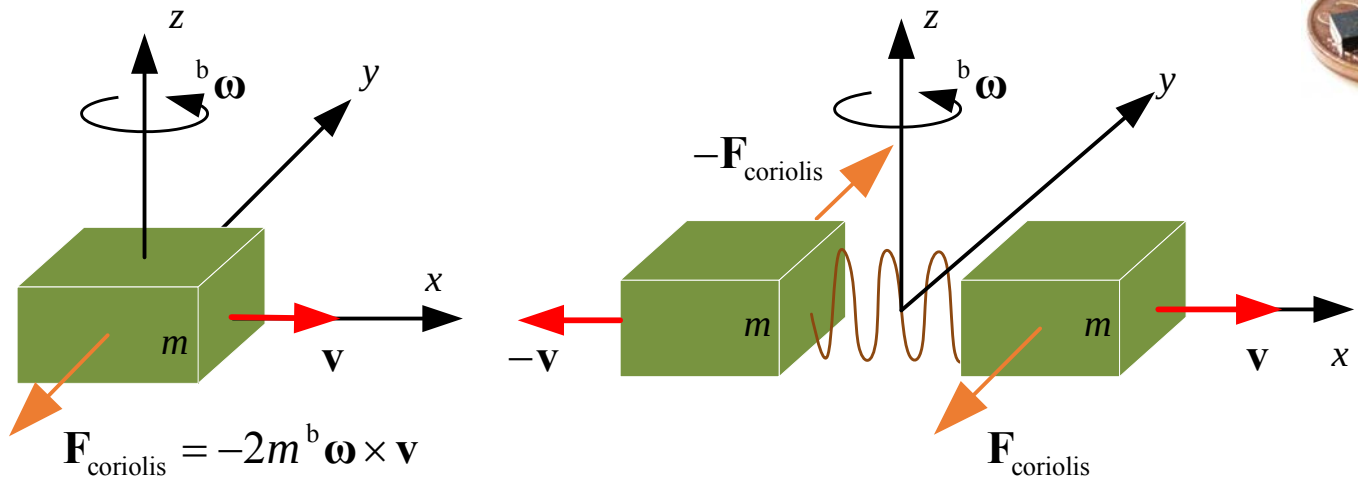

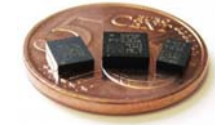

Figure 7.7 Measuring principle of MEMS gyroscope, adapted from http://electroiq.com

- The directions of the accelerations of two masses are opposite but the magnitudes are equal. As a result of the two different forces, the two capacitor plates are forced to generate the capacitance difference. And capacitance difference is proportional to the angular velocity.
- While the change of acceleration will make the two capacitor plates move at same direction, the angular velocity will not be affected.

2.Three-Axis Gyroscope

☐ Automatic Calibration[1],[2]

(1)Error model

There exist some errors in the production and installation process of three-axis gyroscope. Thus the calibration process is needed. The error model is shown as follows:

$$ {}^{b}\boldsymbol{\omega}_{m} = \mathbf{T}_{g}\mathbf{K}_{g}\left({}^{b}\boldsymbol{\omega}'_{m} + \mathbf{b}'_{g}\right) $$

Three-Axis angular velocity after calibration

$$ \mathbf{T}_{g} = \begin{bmatrix} 1 & \Delta\psi_{g} & -\Delta\theta_{g} \\ -\Delta\psi_{g} & 1 & \Delta\phi_{g} \\ \Delta\theta_{g} & -\Delta\phi_{g} & 1 \end{bmatrix} \quad \mathbf{K}_{g} = \begin{bmatrix} s_{gx} & 0 & 0 \\ 0 & s_{gy} & 0 \\ 0 & 0 & s_{gz} \end{bmatrix} \quad \mathbf{b}'_{g} = \begin{bmatrix} b'_{gx} \\ b'_{gy} \\ b'_{gz} \end{bmatrix} $$

Tiny rotation

Scale factor

Three-Axis angular velocity before calibration

bias

2.Three-Axis Gyroscope

☐ Automatic Calibration

(2)Calibration Principle

Principle: The fundamental principle is that the integration of angular velocity by a gyroscope can be used to calculate the angle, which should have the same accuracy as the angle calculated by a calibrated accelerometer.

In order to clarify the calibration process for the gyroscope, a function Ψ is defined as

$$\mathbf{q}'_{\mathrm{a},k+1} = \Psi\left(\Theta_g, \boldsymbol{\omega}'_{\mathrm{m},k:k+1}, \mathbf{q}_{\mathrm{a},k}\right)$$

quaternion obtained, the (k+1)th estimate

unknown parameters of gyroscope

angular velocities between kth and (k+1)th acceleration measurements

Quaternion calculated by calibrated accelerometer, the kth measurement

In Lesson 5: relations between quaternion change rate and angular velocity + RungeKutta method

and

$$\mathbf{\Theta}_{\mathrm{g}} = \left[\Delta\psi_{\mathrm{g}} \quad \Delta\theta_{\mathrm{g}} \quad \Delta\phi_{\mathrm{g}} \quad s_{\mathrm{gx}} \quad s_{\mathrm{gy}} \quad s_{\mathrm{gz}} \quad b'_{\mathrm{gx}} \quad b'_{\mathrm{gy}} \quad b'_{\mathrm{gz}}\right]^{\mathrm{T}}$$

2.Three-Axis Gyroscope

☐ Automatic Calibration

(2)Calibration Principle

The relationship between the quaternion changing rate and the angular velocity of the body can be used to calibrate

$$\dot{\mathbf{q}}_{\mathrm{e}}^{\mathrm{b}}(\mathrm{t})=\frac{1}{2}\begin{bmatrix} 0 & -{}^{\mathrm{b}}\boldsymbol{\omega}^{\mathrm{T}} \\ {}^{\mathrm{b}}\boldsymbol{\omega} & -\left[{}^{\mathrm{b}}\boldsymbol{\omega}\right]_{\times} \end{bmatrix}\mathbf{q}_{\mathrm{e}}^{\mathrm{b}}(\mathrm{t})$$

Then use Runge-Kutta method to achieve integral, get the acceleration after the recursion

the acceleration after the recursion

$$\mathbf{q}'_{\mathrm{a},k} \Rightarrow \mathbf{a}'_{k+1}=\begin{bmatrix} a'_{x_{\mathrm{b}},k+1} \\ a'_{y_{\mathrm{b}},k+1} \\ a'_{z_{\mathrm{b}},k+1} \end{bmatrix}=g\begin{bmatrix} -\sin\theta' \\ \cos\theta'\sin\phi' \\ \cos\theta'\cos\phi' \end{bmatrix}$$

2.Three-Axis Gyroscope

☐ Automatic Calibration

(2)Calibration Principle

It is expected that the calibrated gyroscope should make the estimation $\mathbf{a}'_k$ and measurement ${}^{\mathrm{b}}\mathbf{a}_{\mathrm{m},k}$ by the calibrated accelerometer as close as possible.

$$\mathbf{a}'_k = \mathbf{h}_{\mathrm{g}}\left(\Theta_{\mathrm{g}}, {}^{\mathrm{b}}\omega'_{\mathrm{m},k-1:k}, {}^{\mathrm{b}}\mathbf{a}_{\mathrm{m},k-1}\right)$$

According to this principle, the following optimization is given as

$$\Theta_{\mathrm{g}}^{*} = \arg\min_{\Theta_{\mathrm{g}}} \sum_{k=1}^{M}\left(\mathbf{h}_{\mathrm{g}}\left(\Theta_{\mathrm{g}}, {}^{\mathrm{b}}\omega'_{\mathrm{m},k-1:k}, {}^{\mathrm{b}}\mathbf{a}_{\mathrm{m},k-1}\right) - {}^{\mathrm{b}}\mathbf{a}_{\mathrm{m},k}\right)^{2}$$

Function that can estimate the acceleration based only on the last acceleration and angular velocities

2.Three-Axis Gyroscope

☐ Automatic Calibration

(3)Calibration Results

- Data source： IMU on PIXHAWK, data is collected through analyzing Mavlink protocol via a series bus. And with acceleration data calibrated.
- Calibration result：

$$\mathbf{T}_g = \begin{bmatrix} 1 & 0.1001 & -0.1090 \\ -0.1001 & 1 & 0.1002 \\ 0.1090 & -0.1002 & 1 \end{bmatrix}, \mathbf{K}_g = \begin{bmatrix} 1 & 0 & 0 \\ 0 & 1 & 0 \\ 0 & 0 & 1 \end{bmatrix}, \mathbf{b}'_g = \begin{bmatrix} 0.2001 \\ 0.2002 \\ 0.2004 \end{bmatrix} \times 10^{-3}$$

2.Three-Axis Gyroscope

☐ Automatic Calibration

(3)Calibration Results $\mathbf{Dist}_{\mathrm{g}} \triangleq \left(\mathbf{h}_{\mathrm{g}}\left(\Theta_{\mathrm{g}}, {}^{\mathrm{b}}\omega'_{\mathrm{m},k-1:k}, {}^{\mathrm{b}}\mathbf{a}_{\mathrm{m},k-1}\right) - {}^{\mathrm{b}}\mathbf{a}_{\mathrm{m},k}\right)^2$

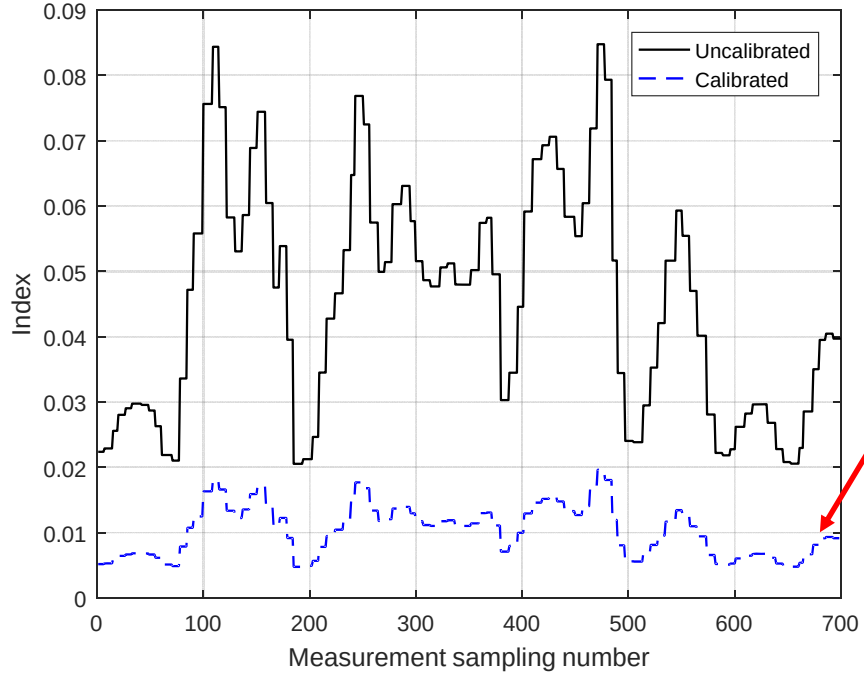

The error become smaller after calibration

Figure 7.8 Calibration error of gyroscope

2.Three-Axis Gyroscope

☐ Measurement Model

MEMS gyroscopes are fixed to the body, which can measure angular velocities along different axes. So, the measurement ${}^{b}\boldsymbol{\omega}_m \in \mathbb{R}$ is denoted as

$$ {}^{b}\boldsymbol{\omega}_m = {}^{b}\boldsymbol{\omega} + \mathbf{b}_g + \mathbf{n}_g $$

Angular velocity after calibration — True value of angular velocity — Drift error — GWN

Furthermore, the drift error is considered to have the following model

$$ \dot{\mathbf{b}}_g = \mathbf{n}_{\mathbf{b}_g} $$

where $\mathbf{n}_{\mathbf{b}_g} \in \mathbb{R}^3$ is often considered as GWN.

3.Three-Axis Magnetometer

☐ Fundamental Principle

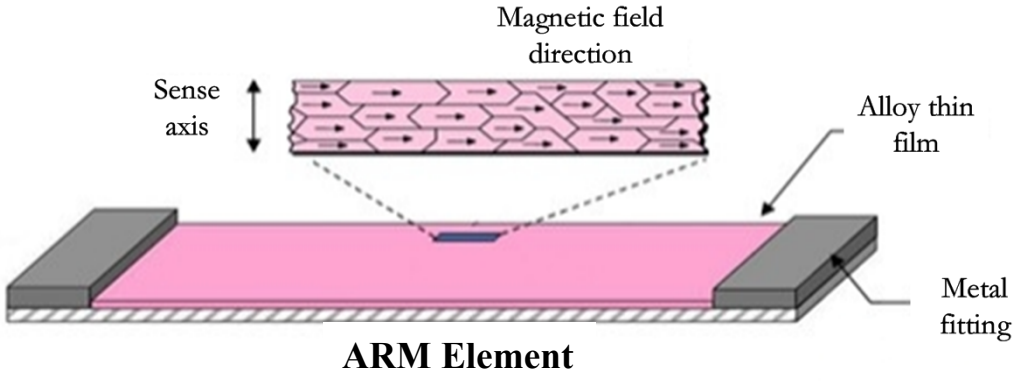

Figure 7.9 anisotropic magnetoresistances,

The magnetometer uses three mutually perpendicular magneto-resistive sensors, and each axial sensor detects the geomagnetic field strength in that direction.

One way is to use an alloy material having a crystalline structure. They are very sensitive to the external magnetic field, magnetic field strength changes will lead to magnetoresistive sensor resistance changes.

3.Three-Axis Magnetometer

☐ Fundamental Principle

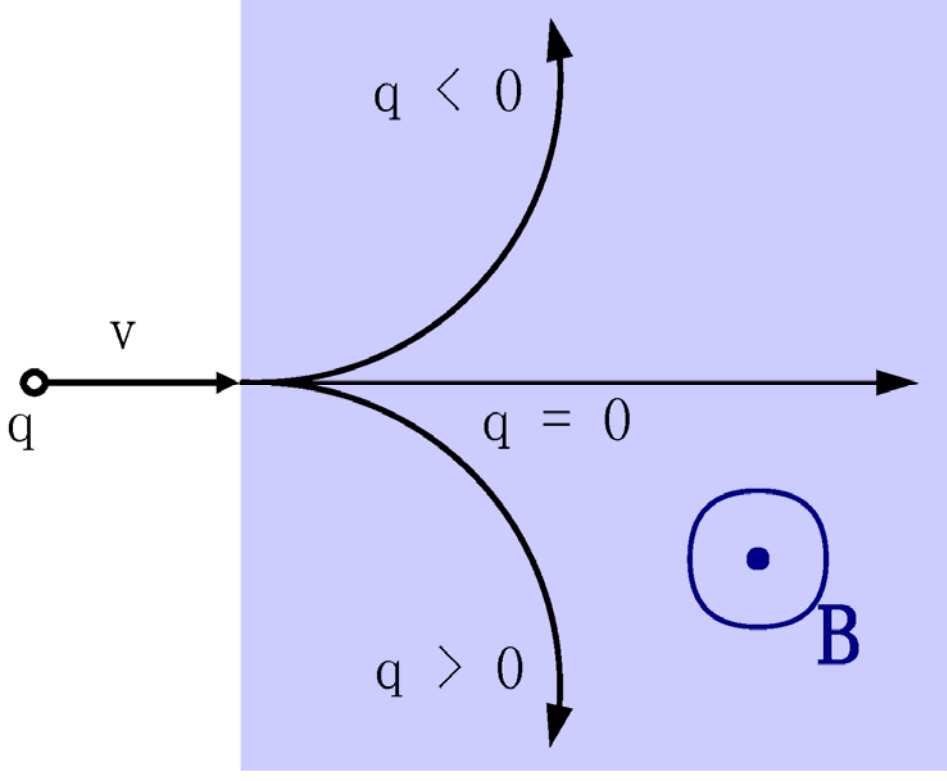

Figure 7.10 Principle of Lorentz Force

Magnetic field direction B points to the outside,q is a charged particle

- Three-axis magnetometer can also use Lorentz force principle, the current flow through the magnetic field to generate force, and generate capacitance changes.

3.Three-Axis Magnetometer

☐ Automatic Calibration[1],[2]

(1)Error Model

There exist some errors in the production and installation process of three-axis magnetometer. And magnetometer is easy to be influenced by surrounding components. Error model is shown as

$$ {}^{b}\mathbf{m}_{m} = \mathbf{T}_{m}\mathbf{K}_{m}\left({}^{b}\mathbf{m}'_{m} + \mathbf{b}'_{m}\right) $$

Calibrated three-axis magnetic induction

$$ \mathbf{T}_{m} = \begin{bmatrix} 1 & \Delta\psi_{m} & -\Delta\theta_{m} \\ -\Delta\psi_{m} & 1 & \Delta\phi_{m} \\ \Delta\theta_{m} & -\Delta\phi_{m} & 1 \end{bmatrix} \quad \mathbf{K}_{m} = \begin{bmatrix} s_{mx} & 0 & 0 \\ 0 & s_{my} & 0 \\ 0 & 0 & s_{mz} \end{bmatrix} $$

three-axis magnetic induction before calibration

$$ \mathbf{b}'_{m} = \begin{bmatrix} b'_{mx} \\ b'_{my} \\ b'_{mz} \end{bmatrix} $$

3.Three-Axis Magnetometer

☐ Automatic Calibration

(2)Calibration Principle

Principle: The magnetic induction keeps constant with different attitude of magnetometer, that is, $\left\| {}^{\mathrm{b}}\mathbf{m}_{\mathrm{m},k} \right\|^2 = 1, k = 1, 2, \ldots, \mathrm{M}$.

In order to calibrate, the following parameters are needed to be estimated.

$$\Theta_{\mathrm{m}} \triangleq \begin{bmatrix} \Delta\psi_{\mathrm{m}} & \Delta\theta_{\mathrm{m}} & \Delta\phi_{m} & s_{\mathrm{mx}} & s_{\mathrm{my}} & s_{\mathrm{mz}} & b'_{\mathrm{mx}} & b'_{\mathrm{my}} & b'_{\mathrm{mz}} \end{bmatrix}^{\mathrm{T}}$$

The function is defined as

$$\mathbf{h}_{\mathrm{m}}\left(\Theta_{\mathrm{m}}, {}^{\mathrm{b}}\mathbf{m}'_{\mathrm{m}}\right) \triangleq \mathbf{T}_{\mathrm{m}}\mathbf{K}_{\mathrm{m}}\left({}^{\mathrm{b}}\mathbf{m}'_{\mathrm{m}} + \mathbf{b}'_{\mathrm{m}}\right)$$

According to this principle, the following optimization is given

$$\Theta_{\mathrm{m}}^{*} = \arg\min_{\Theta_{\mathrm{m}}} \sum_{k=1}^{M} \left(\left\| \mathbf{h}_{\mathrm{m}}\left(\Theta_{\mathrm{m}}, {}^{\mathrm{b}}\mathbf{m}'_{\mathrm{m},k}\right) \right\| - 1 \right)^2$$

3.Three-Axis Magnetometer

☐ Automatic Calibration

(3) Calibration Result

- Data source： IMU on PIXHAWK, data is collected through analyzing Mavlink protocol via a series bus.
- Calibration result：

$$\mathbf{T}_{\mathrm{m}}=\begin{bmatrix}1 & -0.0026 & 0.0516\\ 0.0026 & 1 & -0.0156\\ -0.0516 & 0.0156 & 1\end{bmatrix}\ \mathbf{K}_{\mathrm{m}}=\begin{bmatrix}0.9999 & 0 & 0\\ 0 & 1 & 0\\ 0 & 0 & 0.9999\end{bmatrix}\ \mathbf{b}'_{\mathrm{m}}=\begin{bmatrix}-0.3223\\ -0.1280\\ 0.1589\end{bmatrix}\times 10^{-5}$$

3.Three-Axis Magnetometer

☐ Automatic Calibration

(3) Calibration Result

$$\mathbf{Dist}_{\mathrm{m}} \triangleq \left(\left\| \mathbf{h}_{\mathrm{m}} \left(\Theta_{\mathrm{m}}, {}^{\mathrm{b}}\mathbf{m}'_{\mathrm{m},k} \right) \right\| - 1 \right)^2$$

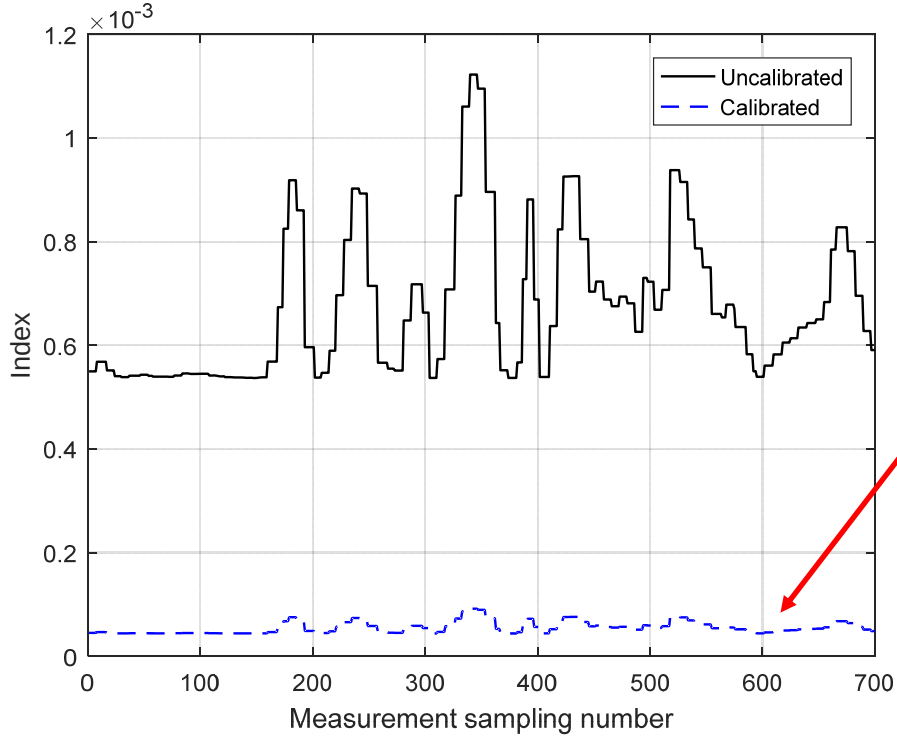

The error become smaller after calibration

Figure 7.11 Calibration error of gyroscope

3.Three-Axis Magnetometer

☐ Measurement Model

The magnetometer is aligned with the body, which can measure magnetic field intensity ${}^{b}\mathbf{m}_{m} \in \mathbb{R}^{3}$ along different axes.

$$ {}^{b}\mathbf{m}_{m} = \mathbf{R}_{e}^{b} \cdot {}^{e}\mathbf{m} + \mathbf{b}_{m} + \mathbf{n}_{m} $$

Calibrated magnetic field intensity

Rotation matrix

Real magnetic field

Drift

GWN

Furthermore, the drift error $\mathbf{b}_{m} \in \mathbb{R}^{3}$ can be considered as

$$ \dot{\mathbf{b}}_{m} = \mathbf{n}_{\mathbf{b}_{m}} $$

And $\mathbf{n}_{\mathbf{b}_{m}} \in \mathbb{R}^{3}$ is considered as GWN.

4. Ultrasonic Range Finder

☐ Fundamental Principle

Ultrasound is sound with a frequency greater than the upper limit of human hearing (greater than 20 kHz). With good directivity and powerful penetrability, ultrasonic is widely used in ranging speed or scale, etc. Therefore, when the time between the ultrasonic sound signal emitting and receiving Δt is known, and v is speed of sound, the distance between range finder and object d is $d = v\Delta t/2$.

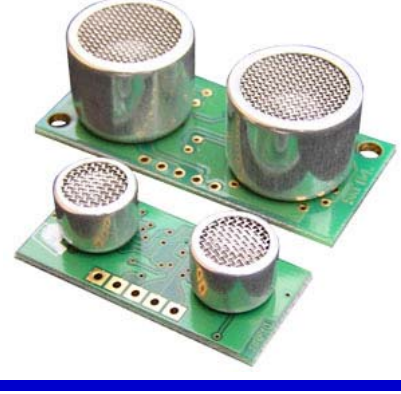

4. Ultrasonic Range Finder

☐ Fundamental Principle

Ultrasonic range finder also has some shortcomings. First, its measurement range is small. Second, as shown, a soft object or an object at a specific angle to the sensor may reflect less or even no reflected waves.

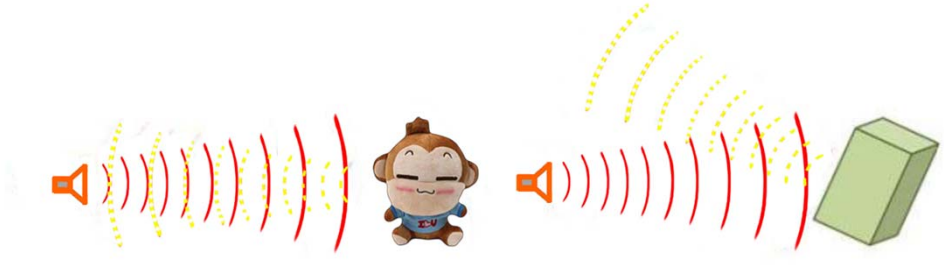

Figure 7.12 Little or no echo reflected from soft objects or at an angle relative to a transducer.

4. Ultrasonic Range Finder

Calibration

These measurements are used for position control. The slight deviations will not cause significant performance degradation to multicopters. Therefore, the deviation of these sensors can be corrected by online state estimation when multicopters are in the air.

Measurement Model

Ultrasonic range finders are typically used to measure the relative height. It is often mounted at the bottom of a multicopter and faces downward. The distance measured by the sensor is $d_{\mathrm{SONAR}} \in \mathbb{R}_+$, and the true height from the ground is denoted as

$$d_{\mathrm{SONAR}} = -\frac{1}{\cos\theta\cos\phi} p_{z_e} + n_{d_{\mathrm{SONAR}}}$$

where $\theta, \phi \in \mathbb{R}$ denote the pitch angle and the roll angle, $n_{d_{\mathrm{SONAR}}} \in \mathbb{R}$ is GWN. If the ultrasonic range finder has a drift error, then its model can be extended similar to the models mentioned before.

5. Barometer

☐ Fundamental Principle

The piezoelectric barometers are often used in multicopters. Barometers are intended to measure the atmospheric pressure, the corresponding altitude, or relative altitude by subtracting two altitudes. Because atmosphere pressure can be easily influenced by wind, barometer can only get an approximate height.

☐ Calibration

These measurements are used for position control. The slight deviations will not cause significant performance degradation to multicopters. Therefore, the deviation of these sensors can be corrected by online state estimation when multicopters are in the air.

5.Barometer

☐ Measurement Model

Barometers are used to measure the absolute height or the relative altitude. The altitude is denoted as

$$d_{\mathrm{BARO}} = -p_{z_e} + b_{d_{\mathrm{BARO}}} + n_{d_{\mathrm{BARO}}}$$

Height measured by barometer

Real height

Drift error

GWN

Drift error $b_{d_{\mathrm{BARO}}} \in \mathbb{R}$ can be considered as

$$\dot{b}_{d_{\mathrm{BARO}}} = n_{b_{d_{\mathrm{BARO}}}}$$

where $n_{b_{d_{\mathrm{BARO}}}} \in \mathbb{R}$ is the GWN.

6. 2D Laser Range Finder

☐ Fundamental Principle

2D laser scanner can be used as a range finder which uses a laser beam to determine the distance. The most common form of laser range finders operates based on the Time of Flight (ToF) principle. A laser pulse is sent in a narrow beam towards the object and the time is measured by the pulse to be reflected off the target and returned to the transmitter. 2D laser rangefinder scanning laser ranging system can achieve a range of 360 degrees, resulting in space where the plane point cloud map information for mapping, robot navigation, object / environmental modeling applications.

☐ Calibration

Because 2D laser scanners are often used for height measurement and obstacle avoidance, the slight deviation of these will not cause significant performance degradation of the aircraft. Thus, these sensors are generally accurate.

6. 2D Laser Range Finder

Measurement Model

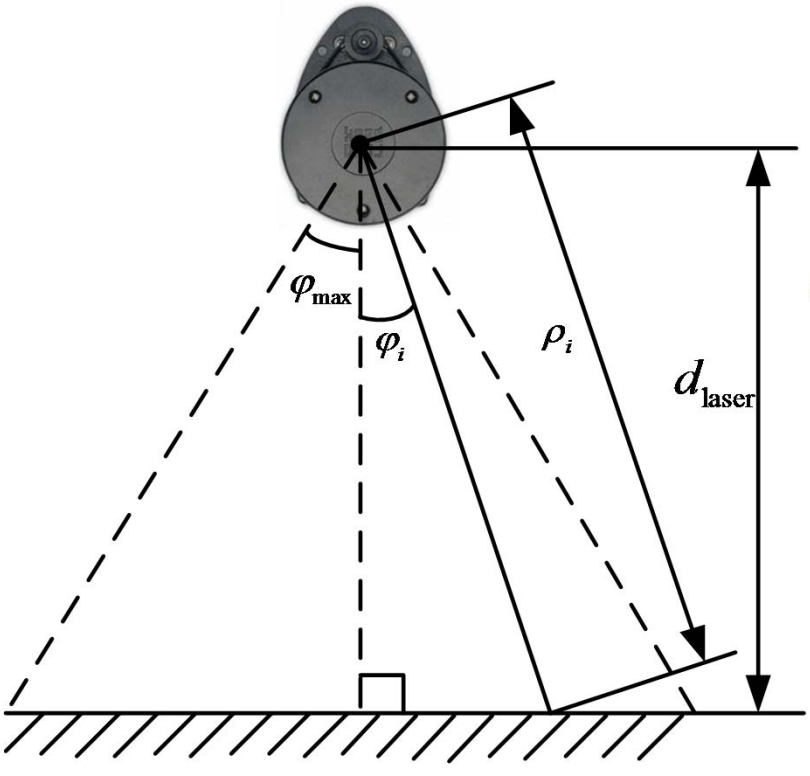

Figure 7.13 The principle of ranging

The height from ground measured by the 2D laser range finder is shown as follows

$$d_{\text{laser}} = \frac{1}{M}\sum_{i=1}^{M}\rho_i \cos\varphi_i = \frac{-1}{\cos\theta\cos\phi} p_{z_e} + n_{d_{\text{laser}}}$$

where $\rho_i \in \mathbb{R}$ and $\varphi_i \in [-\varphi_{\max}, \varphi_{\max}]$ are the value of distance measured by the range finder and the corresponding angle, respectively; n denotes the number of samples, θ, ϕ denote the pitch angle and roll angle, $n_{d_{\text{laser}}} \in \mathbb{R}$ denotes GWN.

6. 2D Laser Range Finder

☐ Supplement(LiDAR)

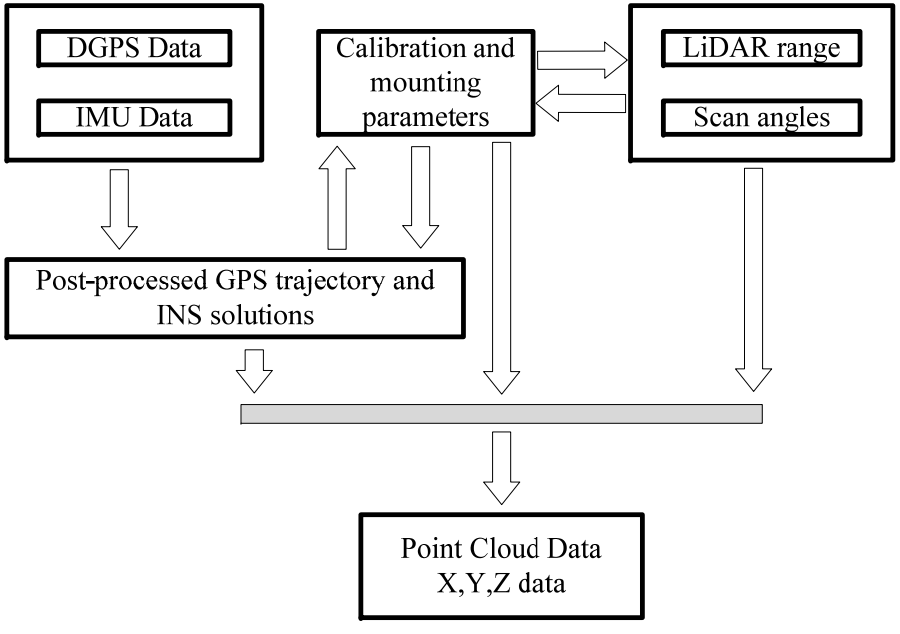

Figure 7.14 Process of producing point cloud

LiDAR, GPS and IMU devices can generate point clouds. The point cloud data contains spatial three-dimensional information and laser intensity information. Artifacts, covering plants, etc., can be removed from these original digital surface models by applying classification techniques to obtain a digital elevation model and to obtain the height of the ground cover at the same time.

6. 2D Laser Range Finder

☐ Supplement(LiDAR)

Figure 7.15 LiDAR of Velodyne company and multicopter with LiDAR

The performance of LiDAR depends on weight, scale, power, horizontal viewing angle, and vertical viewing angle, the number of scanning dot per second, scanning frequency, identification accuracy and number of channels. For example, the weight of VLP-16 from Velodyne Company is only 0.83 kg. Scanning radius scale is 100m. The power is 8W. Horizontal viewing angle is 360°. Vertical viewing angle is ±15°. The number of scanning dots is up to 300000. The scale of scanning frequency is 5~20Hz and so on. Thanks to the miniaturization of LiDAR, it can be carried by multicopters.

6. 2D Laser Range Finder

☐ Supplement(LiDAR)

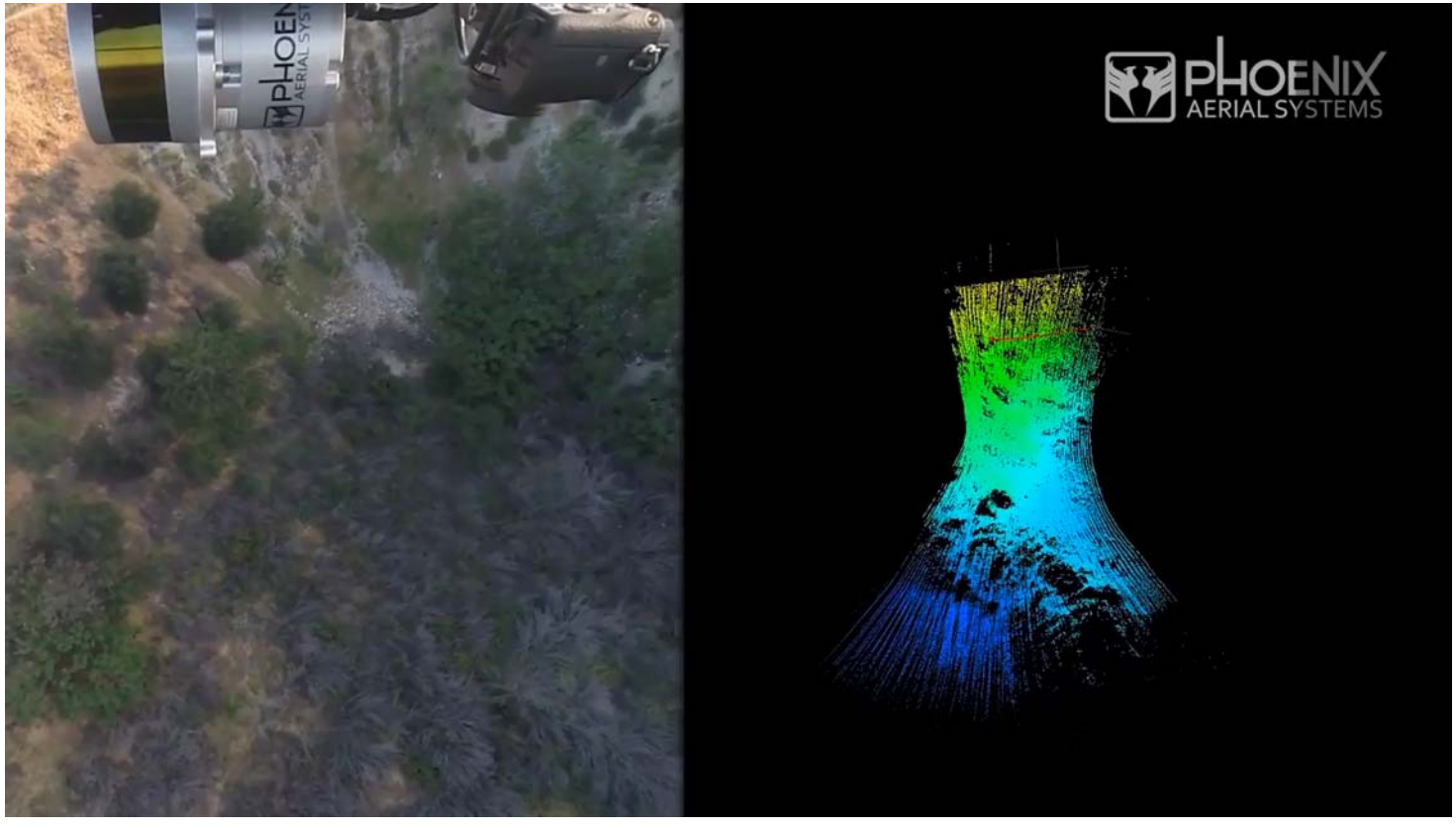

Phoenix Aerial AL3-16 UAV LiDAR Mapping System Overview, https://youtu.be/BhHro_rcgHo

7.GPS

☐ Fundamental Principle

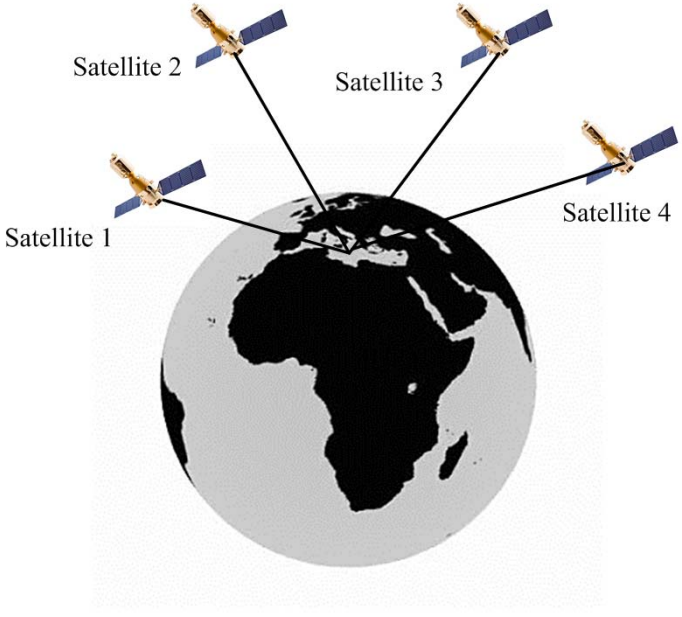

Figure 7.16 GPS schematic diagram

- The Global Positioning System (GPS) consists of a number of satellites in known locations. The basic principle is to measure the distance from the GPS receiver to the satellite, and then determine the position of the GPS receiver by solving the equation.
- For Coarse/Acquisition (C/A) code pseudo-distance measured is called C/A code pseudo-range. The accuracy is about 20 meters. For P code pseudo-distance measured is called P code pseudo-range. Its accuracy is about 2 meters.

7.GPS

Fundamental Principle

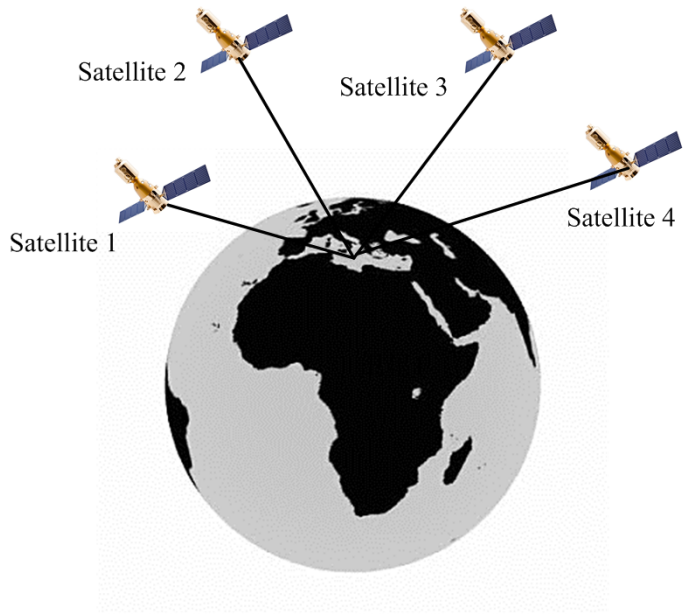

Figure 7.16 GPS schematic diagram

Taking the influence of the ionosphere, troposphere and the clocks into consideration, the basic observation equations of pseudo-range positioning is expressed as

$$\rho = \rho' + c\left(\delta_t + \delta_T\right) + \delta_I$$

Real distance

Pseudo -range

Light speed

Satellite clock error correction given by the satellite navigation

Error correction of the receiver clock relative to the GPS time

Signal propagation delay correction

7.GPS

Fundamental Principle

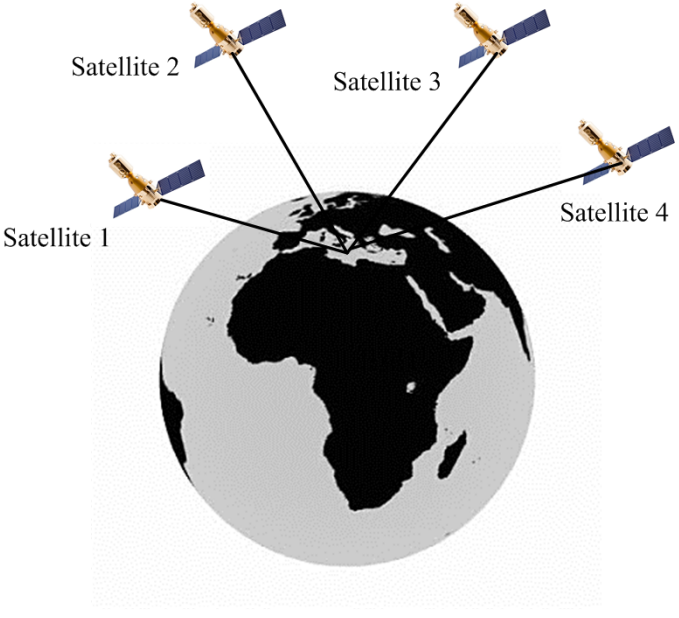

Figure 7.16 GPS schematic diagram

Assuming that the positions of satellites are $\mathbf{p}_{s,k} \in \mathbb{R}^3, k = 1, \cdots, n_s$, and the position of receivers are $\mathbf{p}_r \in \mathbb{R}^3$, and have

$$\left\| \mathbf{p}_{s,k} - \boxed{\mathbf{p}_r} \right\| - \delta_I = \rho'_k + c\left(\delta_{t,k} + \boxed{\delta_T}\right), k = 1, \cdots, n_s$$

Since there are four parameters need to be calculated, the receiver needs to be linked to four satellites at least so that the position can be determined.

7.GPS

☐ Fundamental Principle of DGPS

Differential GPS (DGPS) can improve location accuracy by eliminating the common error. DGPS system consists of base stations, data links and users. It requires a high-quality GPS reference receivers on the known coordinates of the base station, the base station estimates ranging error components of each satellite, and the satellite in the visible range of each satellite forming a correction, the correction value or original observations, sent to all users via the DGPS data links.

7.GPS

Measurement Model

A GPS receiver is mounted on a multicopter to measure its position, ${}^{e}\mathbf{p} \in \mathbb{R}^3$ in the IRF. It can be described as

$$ {}^{e}\mathbf{p}_{\mathrm{GPS}} = {}^{e}\mathbf{p} + \mathbf{b}_{\mathrm{p}} + \mathbf{n}_{\mathrm{p}} $$

The position measured — Real position — Drift error — GWN

Furthermore, drift error $\mathbf{b}_{\mathrm{p}}$ can be modeled as

$$ \dot{\mathbf{b}}_{\mathrm{p}} = \mathbf{n}_{\mathbf{b}_{\mathrm{p}}} $$

where $\mathbf{n}_{\mathbf{b}_{\mathrm{p}}} \in \mathbb{R}^3$ denotes the GWN. GPS and differential GPS both can use the model above, except that they differ in precision, reflected in the drift and noise parameters, as well as their different frequencies.

8.Camera

☐ Fundamental Principle

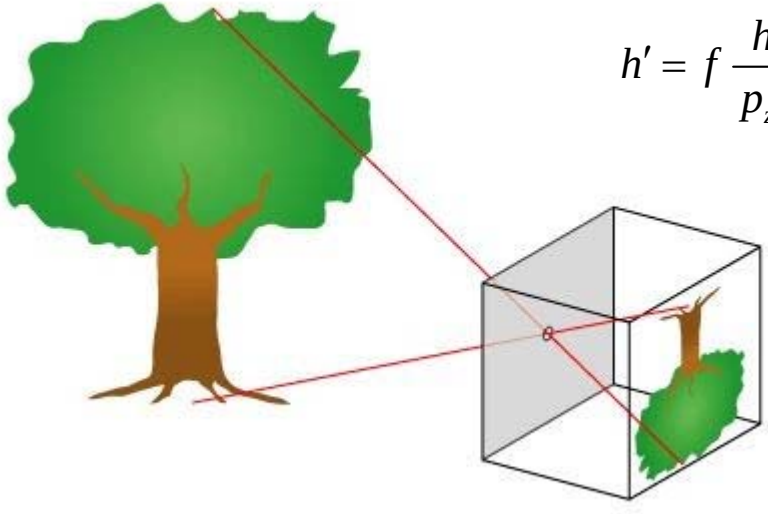

$$h' = f\frac{h}{p_{z_c}}$$

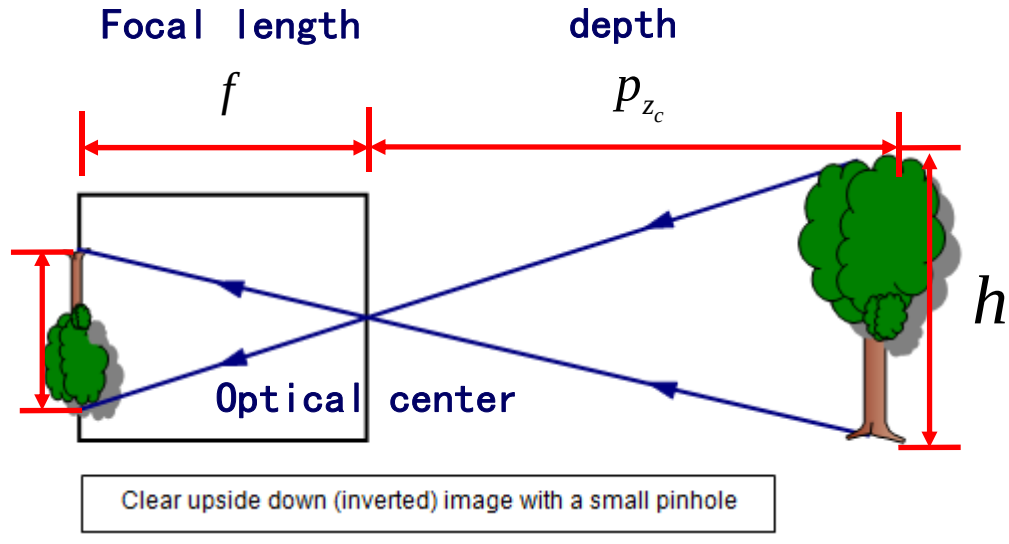

Figure 7.17 Pinhole camera imaging model schematic， http://myworldweb.com/?p=218

8.Camera

Fundamental Principle

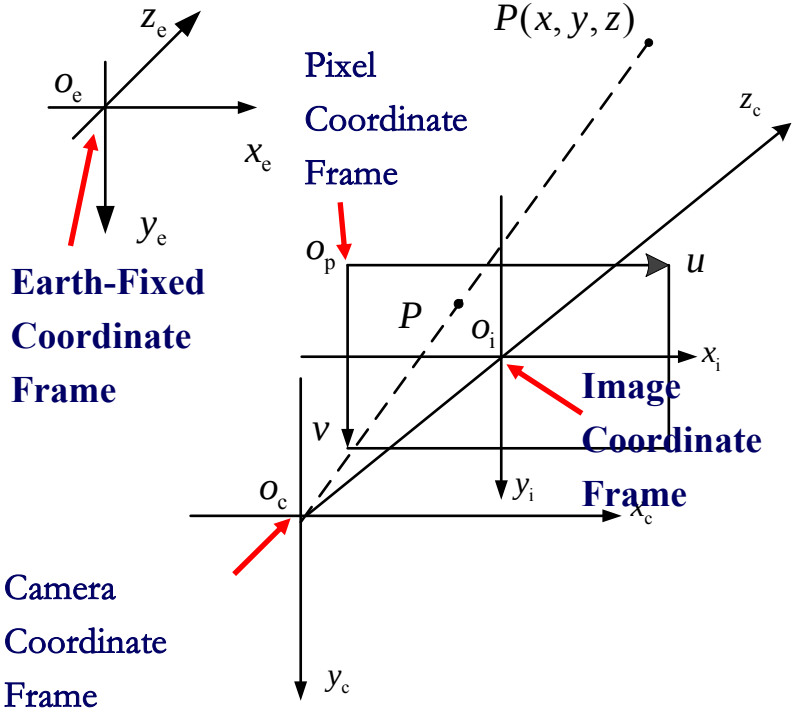

Figure 7.18 Camera Imaging Model

In computer vision, a camera makes the three-dimensional (3D) scene project on a two-dimensional (2D) image plane. For the convenience to study, point P in space in the image position can be modeled as pinhole image model, which is also called as center projection or perspective projection model.

8.Camera

Measurement Model

(1) EFCF to CCF

Rotation Matrix Translation Vector

$$\begin{bmatrix} P_{x_c} \\ P_{y_c} \\ P_{z_c} \\ 1 \end{bmatrix} = \underbrace{\begin{bmatrix} \mathbf{R}_{\mathrm{e}}^{\mathrm{c}} & \mathbf{T} \\ \mathbf{0}_{1\times 3} & 1 \end{bmatrix}}_{\mathbf{M}_2} \begin{bmatrix} P_{x_e} \\ P_{y_e} \\ P_{z_e} \\ 1 \end{bmatrix}$$

(2) CCF to ICF

$$\begin{cases} P_{x_i} = \dfrac{fP_{x_c}}{P_{z_c}} \\ P_{y_i} = \dfrac{fP_{y_c}}{P_{z_c}} \end{cases} \Rightarrow s\begin{bmatrix} P_{x_i} \\ P_{y_i} \\ 1 \end{bmatrix} = \underbrace{\begin{bmatrix} f & 0 & 0 & 0 \\ 0 & f & 0 & 0 \\ 0 & 0 & 1 & 0 \end{bmatrix}}_{\mathbf{P}} \begin{bmatrix} P_{x_c} \\ P_{y_c} \\ P_{z_c} \\ 1 \end{bmatrix} \Rightarrow \begin{cases} u = \dfrac{P_{x_i}}{\mathrm{d}X} + u_0 \\ v = \dfrac{P_{y_i}}{\mathrm{d}Y} + v_0 \end{cases}$$

Millimeter Pixel

8.Camera

Measurement Model

(3) Camera Model

$$s\begin{bmatrix} u \\ v \\ 1 \end{bmatrix} = \begin{bmatrix} \frac{1}{\mathrm{d}X} & 0 & u_0 \\ 0 & \frac{1}{\mathrm{d}Y} & v_0 \\ 0 & 0 & 1 \end{bmatrix} \begin{bmatrix} f & 0 & 0 & 0 \\ 0 & f & 0 & 0 \\ 0 & 0 & 1 & 0 \end{bmatrix} \begin{bmatrix} \mathbf{R}_{\mathrm{e}}^{\mathrm{c}} & \mathbf{T} \\ \mathbf{0}_{1\times 3} & 1 \end{bmatrix} \begin{bmatrix} P_{x_{\mathrm{e}}} \\ P_{y_{\mathrm{e}}} \\ P_{z_{\mathrm{e}}} \\ 1 \end{bmatrix}$$

Pixel Coordinate

Earth-Fixed Coordinate

$$= \underbrace{\begin{bmatrix} \alpha_x & 0 & u_0 & 0 \\ 0 & \alpha_y & v_0 & 0 \\ 0 & 1 & 1 & 0 \end{bmatrix}}_{\boldsymbol{M}_1} \begin{bmatrix} \mathbf{R}_{\mathrm{e}}^{\mathrm{c}} & \mathbf{T} \\ \mathbf{0}_{1\times 3} & 1 \end{bmatrix} \begin{bmatrix} P_{x_{\mathrm{e}}} \\ P_{y_{\mathrm{e}}} \\ P_{z_{\mathrm{e}}} \\ 1 \end{bmatrix} = \mathbf{M}_1\mathbf{M}_2\boldsymbol{X}_{\mathrm{e}} = \mathbf{M}\boldsymbol{X}_{\mathrm{e}}$$

M1 is intrinsic matrix

M2 is extrinsic matrix

where $\alpha_x = \dfrac{f}{\mathrm{d}X}$ is the scale factor of axis u. $\alpha_y = \dfrac{f}{\mathrm{d}Y}$ is the scale factor of axis v.

8.Camera

☐ Intrinsic Parameters Calibration Toolboxes

Toolbox	Description	Website
Computer Vision System Toolbox	The system toolbox supports camera calibration, stereo vision, 3D reconstruction, and 3D point cloud processing.	http://cn.mathworks.com/help/vision/index.html
Camera Calibration Toolbox for Matlab	This is a release of a Camera Calibration Toolbox for MATLAB with a complete documentation, such as fish-eye lens cameras and catadioptric cameras.	http://www.vision.caltech.edu/bouguetj/calib_doc/
Camera Calibration Toolbox for Generic Lenses	This is a camera calibration toolbox for MATLAB which can be used for calibrating several different kinds of cameras.	http://www.ee.oulu.fi/~jkannala/calibration/calibration.html
The DLR Camera Calibration Toolbox	It is followed from the strategic purpose of both upgrading the former CalLab package and at the same time developing a platform independent application.	http://dlr.de/rmc/rm/en/desktopdefault.aspx/tabid-3925/6084_read-9201/
Fully automatic camera and hand to eye calibration	The first part covers a fully automatic calibration procedure and the second covers the calibration of the camera to a robot-arm or an external marker (known as Hand-Eye calibration).	http://www.vision.ee.ethz.ch/software/calibration_toolbox//calibration_toolbox.php
Camera Calibration Tools	This toolbox is a Windows application designed to streamline the camera calibration process. It can be used to capture calibration images from a camera attached to your PC, detect the calibration object and calculate the intrinsic and extrinsic camera parameters.	http://www0.cs.ucl.ac.uk/staff/Dan.Stoyanov/calib/
Omnidirectional Calibration Toolbox	This toolbox can be used to calibrate the camera such as Hyperbolic, Parabolic, Folded Mirror, Spherical, Wide-angle cameras.	http://www.robots.ox.ac.uk/~cmei/Toolbox.html
Camera Calibration Toolbox for Generic Multiple Cameras	This is a camera calibration toolbox for generic multiple cameras. The toolbox can be used to calibrate: (1) two conventional cameras; (2) two fish-eye cameras; (3) two mixed cameras; (4) multiple cameras.	http://quanquan.buaa.edu.cn/CalibrationToolbox.html

9. Conclusion

- In this lesson, fundamental principles of sensors are introduced. Since no other device is needed, these methods are practical.
- Due to installation problems, it is impossible to place all sensors on the Center of Gravity (CoG). So the methods of calibrating the extrinsic parameters need to be further studied.

IMU Calibration Reference

[1] D. Tedaldi, A. Pretto and E. Menegatti. A Robust and Easy to Implement Method for IMU Calibration without External Equipments. 2014 IEEE International Conference on Robotics & ,2014,Hong Kong, China.

[2] E. Dorveaux, D. Vissière, A. P. Martin, and N. Petit. Iterative calibration method for inertial and magnetic sensors. IEEE International Conference on on Decision and Control, 2009, Shanghai, China.

Acknowledgement

Deep thanks go to graduate student

Jianing Fu

Heng Deng

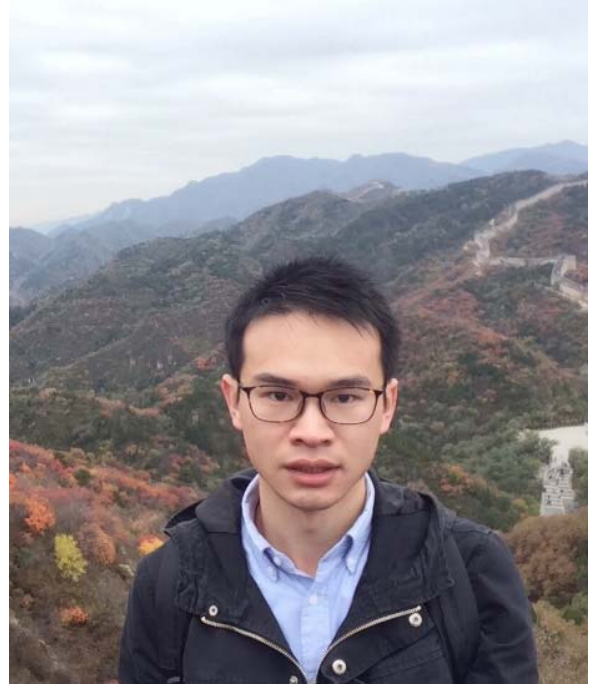

Xunhua Dai

for material preparation.

Thank you!

All course PPTs and resources can be downloaded at
http://rfly.buaa.edu.cn/course

For more detailed content, please refer to the textbook:

Quan, Quan. Introduction to Multicopter Design and Control. Springer, 2017. ISBN: 978-981-10-3382-7.

It is available now, please visit http://
www.springer.com/us/book/9789811033810